



# Simultaneously transmitting and reflecting reconfigurable intelligent surfaces (STAR-RIS) with energy harvesting and adaptive power

Raed Alhamad<sup>1</sup> · Hatem Boujemâa<sup>2</sup>

Received: 15 September 2023 / Revised: 25 September 2023 / Accepted: 29 September 2023 / Published online: 29 October 2023  
© The Author(s), under exclusive licence to Springer-Verlag London Ltd., part of Springer Nature 2023

## Abstract

In this paper, we evaluate and optimize the throughput of STAR-RIS for underlay cognitive radio networks (CRN) with energy harvesting from radio frequency (RF) signals. The secondary source  $S_S$  harvests power from node  $A$  RF signal. Then,  $S_S$  adapts its power to control the interference at primary destination  $P_D$ . The broadcasted signal will be delivered to two users  $U_t$  and  $U_r$  located in the space of transmission and reflection of STAR-RIS in the secondary network. When STAR-RIS is used, the signal to interference plus noise ratio (SINR) at users  $U_t$  and  $U_r$  is maximized by a wise optimization of STAR-RIS phases. STAR-RIS offers a diversity equal to the number of its elements  $N$ . Therefore, when the number of STAR-RIS elements  $N$  is doubled, we get up to 15 dB gain.

**Keywords** STAR-RIS · 6G · CRN · Power adaptation

## 1 Introduction

STAR-RIS allows to transmit data to two users  $U_t$  and  $U_r$  [1–5]. The phases shifts of STAR-RIS are optimized to maximize the SINR at  $U_t$  and  $U_r$  [6–8]. STAR-RIS is a good candidate for 6G communications due to its large throughput and performance enhancement with an increase of number of reflectors  $N$ . STAR-RIS for **non-orthogonal multiple access (NOMA)** was studied in [1–9]. The rate of NOMA using STAR-RIS was analyzed in [1]. A comparison of orthogonal multiple access (OMA) and NOMA was presented in [2, 3]. STAR-RIS with federated learning was given in [4]. Channel estimation for STAR-RIS was investigated in [5]. Signal enhancement for STAR-RIS was studied in [6]. Weighted sum rate optimization was discussed in [7]. The security of STAR-RIS was investigated in [8]. Full-duplex communications using STAR-RIS were suggested in [9]. STAR-RIS using multiple antennas was studied in [10, 11]. Sum rate maximization and resource optimization were

suggested in [12]. STAR-RIS for unmanned aerial vehicle (UAV) was studied in [13, 14]. Performance analysis of wireless communications using STAR-RIS was suggested in [15]. STAR-RIS with correlated antennas was presented in [16]. The outage probability of STAR-RIS was derived in [17, 18]. The coverage probability of STAR-RIS was derived in [19]. The performance of the network was optimized in [20]. The security of uplink NOMA was studied in [21]. The design of STAR-RIS was discussed in [24–29]. The capacity of STAR-RIS with fixed power was derived in [22, 23]. Power allocation was investigated in [24]. The design of NOMA using STAR-RIS was suggested in [25, 26]. Phase design of STAR-RIS was optimized in [27] so that the SINR is maximized at the two studied users. A network with multiple cells was studied in [28]. The security and two-way relaying were studied in [29, 30]. Device-to-device (D2D) communications using STAR-RIS were proposed in [30].

In CRN, primary and secondary users share the same channel. CRN allows larger data rates than non CRN as the throughput is equal to the sum of primary and secondary throughput. In interweave CRN, spectrum sensing is performed to detect a vacant band left unused by primary users. Therefore, secondary users transmit only when primary users are idle and the band is available. In underlay CRN, secondary users transmit over the same channel as primary users and adapt their power to minimize the interference at primary users. In this paper, we evaluate and optimize the through-

✉ Raed Alhamad  
ralhamad@seu.edu.sa

Hatem Boujemâa  
boujemaa.hatem@supcom.tn

<sup>1</sup> Saudi Electronic University, Riyadh, Kingdom of Saudi Arabia

<sup>2</sup> COSIM Lab, Tunis, Tunisia

put of underlay CRN where the secondary source harvests energy from RF signals and adapts its power to control the interference at primary destination. STAR-RIS is between the secondary source and two users  $U_t$  and  $U_r$  so that the signal to interference plus noise ratio (SINR) is maximized. STAR-RIS offers a diversity equal to the number of its elements  $N$  and allows a significant throughput enhancement. Therefore, STAR-RIS is a good candidate for 6G wireless communications.

STAR-RIS with power adaptation was not studied in [1–30]. Therefore, STAR-RIS was not yet proposed for underlay CRN where the secondary source adapts its power to minimize the interference at primary destination. In fact, the transmit power is fixed in [1–30] and cannot be used in underlay CRN. In this paper, it is assumed that  $S_S$  harvests power from the node  $A$  signal. The harvested power is used to broadcast data to two secondary users  $U_t$  and  $U_r$ .  $S_S$  controls the level of interference at  $P_D$  using power adaptation.

- We evaluate the throughput of STAR-RIS when  $S_S$  harvests power from node  $A$  signal. We also consider that  $S_S$  use power adaptation to control the level of interference at  $P_D$ .
- There are two main contributions in this paper. First, we study STAR-RIS for underlay CRN where the secondary source has an adaptive transmit power while the power is fixed in [1–30]. Second, the secondary source does not have a battery that should be recharged as assumed in [1–30]. The secondary source harvests energy from node  $A$  RF signal to be able to transmit data to  $U_t$  and  $U_r$  using STAR-RIS.
- We optimize the throughput by adjusting the harvesting duration.

Next section describes the harvested power. Section 3 computes the throughput of STAR-RIS. Section 4 describes the theoretical and simulation results. Section 5 concludes the article.

## 2 Energy harvesting

The harvested energy is [30]

$$E = P_A \alpha F \varepsilon \mu_0 |h|^2, \quad (1)$$

where  $F$  and  $0 < \alpha F < F$  are frame and harvesting durations,  $P_A$  is the power of node  $A$ ,  $0 < \varepsilon < 1$  is the efficiency of the energy conversion, and  $\sqrt{\mu_0}h$  is channel from  $A$  to  $S_S$ .

The available transmit symbol energy is

$$E_{s,available} = \frac{E}{(1-\alpha)\frac{F}{T_s}} = \beta |h|^2, \quad (2)$$

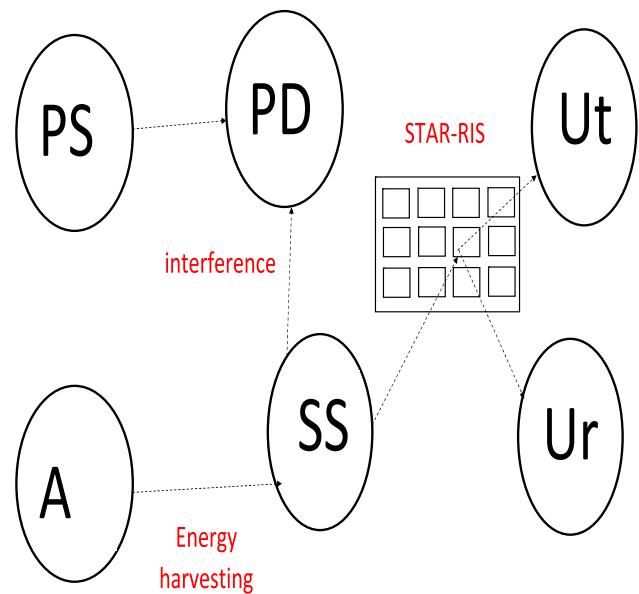


Fig. 1 STAR-RIS for CRN

where  $T_s$  is the symbol period,

$$\beta = \frac{\mu_0 E_A \varepsilon \alpha}{1 - \alpha} \quad (3)$$

where  $E_A = P_A T_s$

We deduce the symbol energy as

$$E_s = \min \left( \frac{T}{|h_{S_S P_D}|^2}, E_{s,available} \right) \quad (4)$$

where  $h_{XY}$  is the channel from  $X$  to  $Y$  and  $T$  is the interference threshold. The generated interference at  $P_D$  is less than  $T$ :  $E_s |h_{S_S P_D}|^2 \leq T$ .  $E_s$  and  $T$  are in Joules,  $F$  and  $T_s$  are in seconds, and all other parameters do not have units.

The cumulative distribution function (CDF) of  $E_s$  is

$$F_{E_s}(x) = 1 - P \left( \min \left( \frac{T}{|h_{S_S P_D}|^2}, E_{s,available} \right) > x \right) \quad (5)$$

We deduce

$$\begin{aligned} F_{E_s}(x) &= 1 - P \left( \frac{T}{|h_{S_S P_D}|^2} > x \right) P(E_{s,available} > x) \\ &= 1 - \left[ 1 - e^{-\frac{T}{x \rho_{S_S P_D}}} \right] e^{-\frac{x}{\beta}} \end{aligned} \quad (6)$$

where  $\rho_{S_S P_D} = E(|h_{S_S P_D}|^2)$ .

## 3 STAR-RIS system model

In Fig. 1, the source  $S_S$  harvests power from node  $A$  RF signal to broadcast data to two users  $U_t$  and  $U_r$ . A STAR-RIS

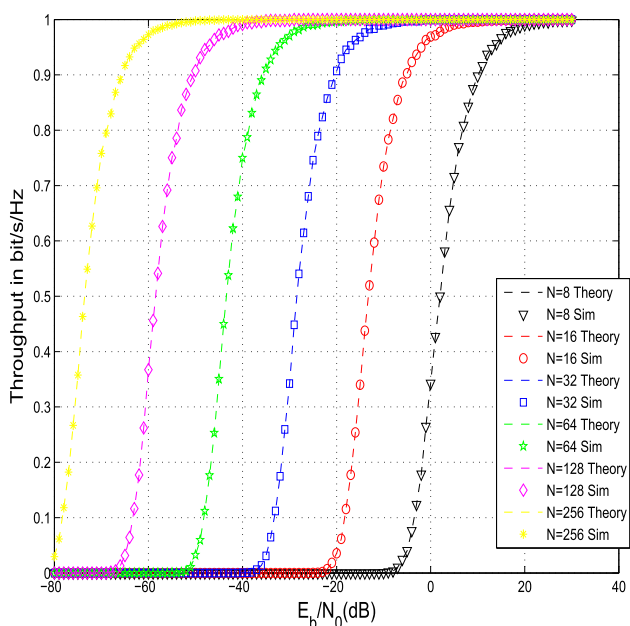


**Fig. 2** Throughput for interference threshold  $T = 1$  and number of STAR-RIS elements  $N = 8, 16, 32, 64, 128, 256$

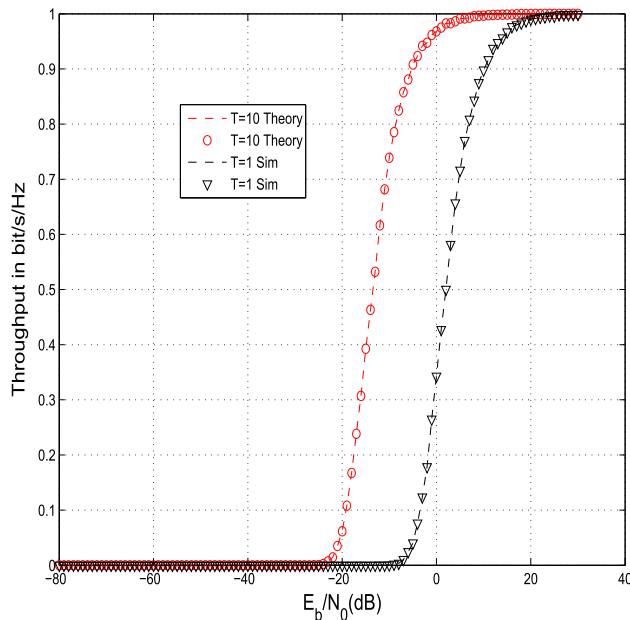


**Fig. 3** Throughput for interference threshold  $T = 1, 10$  and number of STAR-RIS elements  $N = 8$

with  $N$  elements is between the source  $S_S$  and  $U_t, U_r$ . We assume a line-of-sight (LOS) propagation between the secondary source and STAR-RIS and from STAR-RIS to  $U_t$  and  $U_r$  as considered in [1–30]. The transmission and reflection coefficients are  $\eta_n^t e^{j\theta_n^t}$  and  $\eta_n^r e^{j\theta_n^r}$  where  $0 < \theta_n^r, \theta_n^t < 1$  and  $0 < \eta_n^r < 1, 0 < \eta_n^t < 1$  such that  $(\eta_n^r)^2 + (\eta_n^t)^2 = 1$ .  $U_r$  and  $U_t$  are located, respectively, in the space of reflection and transmission of STAR-RIS. The channel between the source  $S_S$  and STAR-RIS is denoted by  $h_n = |h_n| e^{j\phi_{h_n}}$  while the channel between the  $n$ th element of STAR-RIS and user  $U_q$  for  $q = t, r$  is  $g_n^q = |g_n^q| e^{j\phi_{g_n^q}}$ .

The signal at  $U_q$   $q = r, t$  is

$$y_q = \sqrt{E_s \zeta_q} \sum_{n=1}^N g_n^q \eta_n^q e^{j\theta_n^q} h_n x_q + \sqrt{E_s \zeta_{q'}} \sum_{n=1}^N g_n^q \eta_n^q e^{j\theta_n^q} h_n x_{q'} + n_q; \tag{7}$$

where  $q' = r$  when  $q = t$  and  $q' = t$  when  $q = r$ ,  $\zeta_q$  and  $\zeta_{q'}$  are power allocation coefficient for  $U_q$  and  $U_{q'}$  where  $\zeta_q + \zeta_{q'} = 1$ .  $x_q$  (resp.  $x_{q'}$ ) is the symbol of  $U_q$  (resp.  $U_{q'}$ ). The broadcasted signal by  $S_S$  is equal to  $\sqrt{E_s}[\sqrt{\zeta_r} x_r + \sqrt{\zeta_t} x_t]$ .  $n_q$  is Gaussian, zero mean with variance  $N_0$ .

The SNR at  $U_q$  is expressed as

$$\gamma_q = \frac{E_s \zeta_q |\sum_{n=1}^N |g_n^q| |h_n| \eta_n^q \exp(j[\theta_n^q + \phi_{h_n} + \phi_{g_n^q}])|^2}{N_0 + E_s \zeta_{q'} |\sum_{n=1}^N |g_n^q| |h_n| \eta_n^q \exp(j[\theta_n^q + \phi_{h_n} + \phi_{g_n^q}])|^2} \tag{8}$$

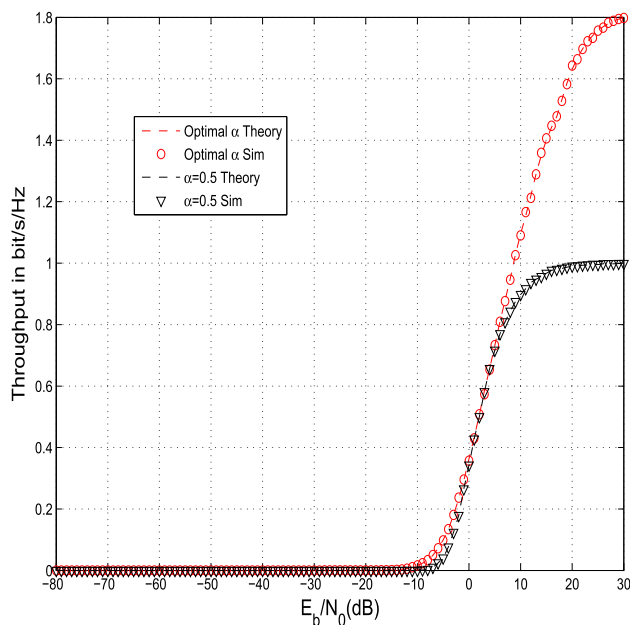


**Fig. 4** Throughput for number of STAR-RIS elements  $N = 8$ , interference threshold  $T = 1$ , optimal harvesting duration  $\alpha$  and  $\alpha = 0.5$

The optimal STAR-RIS phase shifts are chosen so that all reflections have a zero phase  $\theta_n^q + \phi_{h_n} + \phi_{g_n^q} = 0$  [1]. Therefore, we have

$$\theta_n^q = -\phi_{h_n} - \phi_{g_n^q}. \tag{9}$$

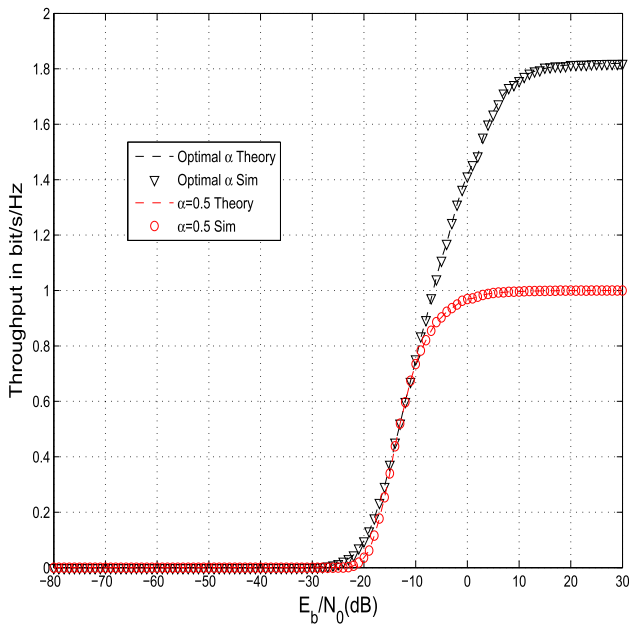


**Fig. 5** Throughput for number of STAR-RIS elements  $N = 16$ , interference threshold  $T = 1$ , optimal harvesting duration  $\alpha$  and  $\alpha = 0.5$

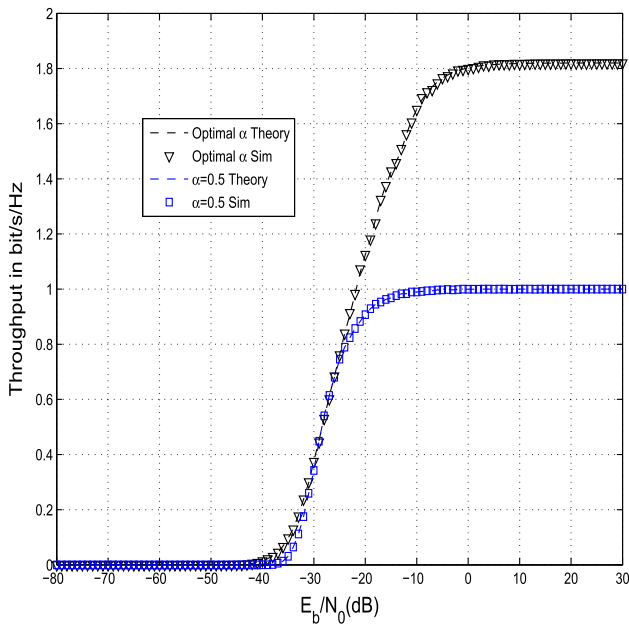


**Fig. 6** Throughput for number of STAR-RIS elements  $N = 32$ , interference threshold  $T = 1$ , optimal harvesting duration  $\alpha$  and  $\alpha = 0.5$

Using (9), the optimal SINR at  $U_q$  is equal to

$$\gamma_q = \frac{E_s \zeta_q A_q^2}{E_s \zeta_q A_q^2 + N_0} \tag{10}$$

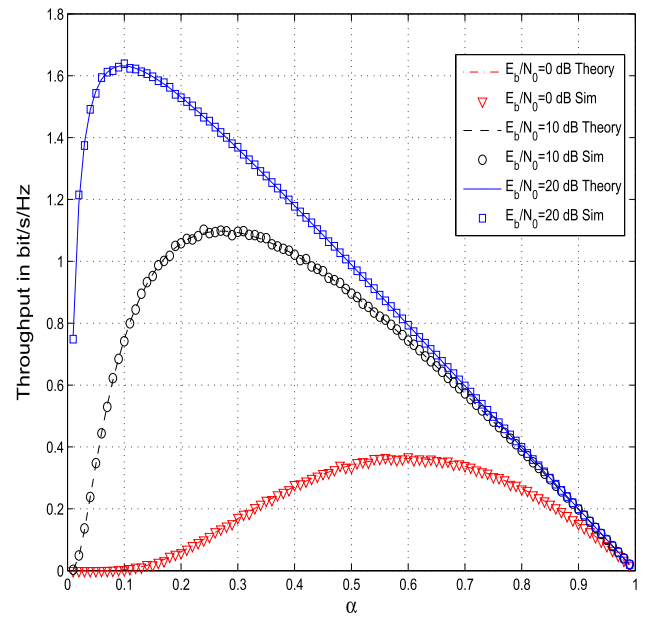


**Fig. 7** Throughput versus harvesting duration  $\alpha$  for number of STAR-RIS elements  $N = 8$  and interference threshold  $T = 1$

where

$$A_q = \sum_{n=1}^N |g_n^q| |h_n| \eta_n^q \tag{11}$$

$A_q$  is Gaussian with mean

$$m_{A_q} = \sum_{n=1}^N \eta_n^q \frac{\pi}{4} \frac{1}{d_{\text{STAR-RIS}, U_q}^{\text{ple}/2} d_{S_s, \text{STAR-RIS}}^{\text{ple}/2}} \tag{12}$$

and variance

$$\sigma_{A_q}^2 = \sum_{n=1}^N (\eta_n^q)^2 \left[ 1 - \frac{\pi^2}{16} \right] \frac{1}{d_{\text{STAR-RIS}, U_q}^{\text{ple}} d_{S_s, \text{STAR-RIS}}^{\text{ple}}} \tag{13}$$

where ple is the path loss exponent and  $d_{XY}$  is the distance from  $X$  to  $Y$ .

Let  $X_q = A_q^2$  and  $Y_q = E_s A_q^2 = E_s X_q$ , the CDF of SINR  $\gamma_q$  is deduced from that of  $Y_q$  as

$$F_{\gamma_q}(x) = F_{Y_q} \left( \frac{N_0 x}{\zeta_q - \zeta_q' x} \right). \tag{14}$$

where  $F_{Y_q}(x)$  is provided in (18).

We have

$$Y_q = E_s X_q \tag{15}$$

where

$$X_q = A_q^2, \tag{16}$$

The CDF of  $X_q$  is

$$F_{X_q}(x) = P(-\sqrt{x} \leq A_q \leq \sqrt{x}) \\ \simeq 0.5 \operatorname{erfc}\left(\frac{-\sqrt{x} - m_{A_q}}{\sqrt{2}\sigma_{A_q}}\right) - 0.5 \operatorname{erfc}\left(\frac{\sqrt{x} - m_{A_q}}{\sqrt{2}\sigma_{A_q}}\right) \quad (17)$$

By derivation, the probability density function (PDF) of  $X_q$  is

$$p_{X_q}(x) \simeq \sqrt{\frac{1}{8\pi\sigma_{A_q}^2 x}} e^{-\frac{[\sqrt{x} + m_{A_q}]^2}{2\sigma_{A_q}^2}} \\ + \sqrt{\frac{1}{8\pi\sigma_{A_q}^2 x}} e^{-\frac{[\sqrt{x} - m_{A_q}]^2}{2\sigma_{A_q}^2}}. \quad (18)$$

The CDF of  $Y_q$  is evaluated as

$$F_{Y_q}(y) = \int_0^{+\infty} F_{E_s}\left(\frac{y}{x}\right) p_{X_q}(x) dx, \quad (19)$$

The packet error probability (PEP) is deduced from the CDF of the SINR  $\gamma_q$ ,  $F_{\gamma_q}(x)$ , using the waterfall threshold  $w_0$ : [31]

$$\operatorname{PEP}_q < F_{\gamma_q}(w_0), \quad (20)$$

In this paper, we use the upper bound (20) to evaluate the  $\operatorname{PEP}_q$  at  $U_q$ .  $w_0$  is defined as [31]

$$w_0 = \int_0^{+\infty} [1 - \operatorname{SEP}(z)]^{PL} dz, \quad (21)$$

$\operatorname{SEP}$  is the symbol error probability [32]

$$\operatorname{SEP}(z) = 2 \left(1 - \frac{1}{\sqrt{Q}}\right) \operatorname{erfc}\left(\sqrt{\frac{3z}{Q-1}}\right) \quad (22)$$

$PL$  and  $Q$  are packet and constellation size.

The throughput is

$$\operatorname{Thr}_q(\alpha) = (1 - \alpha)[1 - \operatorname{PEP}_q(\alpha)], \quad (23)$$

In Eq. (23),  $0 < \alpha < 1$  gives the harvesting duration  $\alpha F$  where  $F$  is the frame duration in seconds. The throughput is maximized as

$$\operatorname{Thr}_q^{\max} = \max_{0 < \alpha < 1} \operatorname{Thr}_q(\alpha). \quad (24)$$

## 4 Results

We plotted the throughput for  $\varepsilon = 0.5$ ,  $d_{S_S, \text{STAR-RIS}} = 1$ ,  $d_{\text{STAR-RIS}, U_t} = 1$ ,  $d_{\text{STAR-RIS}, U_r} = 1.5$ ,  $PL = 500$ ,  $ple = 3$ . The other parameters are  $\zeta_q = 0.8 = 1 - \zeta_q$ ,  $\eta_n^t = \eta_n^r = \frac{1}{\sqrt{2}}$ .

Figure 2 shows the throughput for CRN with adaptive power for  $T = 1$ ,  $\alpha = 0.5$ ,  $T = 1$  and  $N = 8, 16, 32, 64, 128, 256$ . When STAR-RIS is used, the SINR at users  $U_t$  and  $U_r$  is maximized by a wise optimization of STAR-RIS phases. STAR-RIS offers a diversity equal to the number of its elements  $N$ . Therefore, when the number of STAR-RIS elements  $N$  is doubled, we get 15 dB diversity gain.

Figure 3 depicts the throughput for  $T = 10, 1, N = 8$ , and  $\alpha = 0.5$ . We observe the throughput improves for  $T = 10$  as  $S_S$  can increase its power. The numerical results are close to the simulation results and confirms that our derivations are correct.

Figures 4, 5, and 6 depict the throughput for  $N = 8, 16, 32, T = 1$ . The obtained throughput for optimal  $\alpha$  is better than  $\alpha = 0.5$  since harvesting duration optimization offers an important increase in throughput.

Figure 7 depicts the throughput versus  $\alpha$  for  $N = 8$  and  $T = 1$ . Throughput is concave and can be maximized.

## 5 Conclusion

In this article, we proposed the use of STAR-RIS for underlay cognitive radio networks. We studied the throughput of STAR-RIS with energy harvesting. Power adaptation is used by the secondary source to control the level of interference at  $P_D$ . The secondary source transmits data to two users  $U_t$  and  $U_r$ . We obtained 15 dB gain when the number of reflectors is doubled. The obtained results can be applied for underlay cognitive radio networks. As a perspective, we can study STAR-RIS with multipath propagation.

**Author Contributions** It is the contribution of Raed Alhamad and Hatem Boujemaa.

**Funding** This paper was funded by SEU.

**Data availability** Material and data are not available.

**Code Availability** Custom code and software application are not available.

## Declarations

**Conflict of interest** There is no conflict of interest for this article.



## References

1. Zhao, B., Zhang, C., Yi, W., Liu, Y.: Ergodic rate analysis of STAR-RIS aided NOMA systems. *IEEE Commun. Lett.* **26**, 2297–2301 (2022)
2. Mu, X., Liu, Y., Guo, L., Lin, J., Schober, R.: Simultaneously transmitting and reflecting (STAR) RIS aided wireless communications. *IEEE Trans. Wirel. Commun.* **21**(5), 3083–3098 (2022)
3. Wu, C., Liu, Y., Mu, X., Gu, X., Dobre, O.A.: Coverage characterization of STAR-RIS networks: NOMA and OMA. *IEEE Commun. Lett.* **25**(9), 3036–3040 (2021)
4. Ni, W., Liu, Y., Eldar, Y.C., Yang, Z., Tian, H.: Enabling ubiquitous non-orthogonal multiple access and pervasive federated learning via STAR-RIS. In: 2021 IEEE Global Communications Conference (GLOBECOM) (2021)
5. Wu, C., You, C., Liu, Y., Gu, X., Cai, Y.: Channel estimation for STAR-RIS-aided wireless communication. *IEEE Commun. Lett.* **26**(3), 652–656 (2022)
6. Hou, T., Wang, J., Liu, Y., Sun, X., Li, A., Ai, B.: A joint design for STAR-RIS enhanced NOMA-CoMP networks: a simultaneous-signal-enhancement-and-cancellation-based (SSECB) design. *IEEE Trans. Veh. Technol.* **71**(1), 1043–1048 (2022)
7. Niu, H., Chu, Z., Zhou, F., Xiao, P., Al-Dhahir, N.: Weighted sum rate optimization for STAR-RIS-assisted MIMO system. *IEEE Trans. Veh. Technol.* **71**(2), 2122–2127 (2022)
8. Han, Y., Li, N., Liu, Y., Zhang, T., Tao, X.: Artificial noise aided secure NOMA communications in STAR-RIS networks. *IEEE Wirel. Commun. Lett.* **11**(6), 1191–1195 (2022)
9. Perera, P.P., Warnasooriya, V.G., Kudathanthirige, D., Suraweera, H.A.: Sum rate maximization in STAR-RIS assisted full-duplex communication systems. In: ICC 2022-IEEE International Conference on Communications (2022)
10. Zuo, J., Liu, Y., Ding, Z., Lingyang S.: Simultaneously transmitting and reflecting (STAR) RIS assisted NOMA systems (2021). In: IEEE Global Communications Conference (GLOBECOM)
11. Mu, X., Liu, Y., Xu, J., Guo, L., Lin, J.: Joint beamforming optimization for simultaneously transmitting and reflecting (STAR) RIS aided communications: (invited paper). In: 2021 55th Asilomar Conference on Signals, Systems, and Computers (2021)
12. Wu, C., Mu, X., Liu, Y., Gu, X., Wang, X.: Resource allocation in STAR-RIS-aided networks: OMA and NOMA. *IEEE Trans. Wirel. Commun.* **21**(9), 7653–7667 (2022)
13. Zhang, Q., Zhao, Y., Li, H., Hou, S., Song, Z.: Joint optimization of STAR-RIS assisted UAV communication systems. *IEEE Wirel. Commun. Lett.* **11**, 2390–2394 (2022)
14. Zhao, J., Zhu, Y., Mu, X., Cai, K., Liu, Y., Hanzo, L.: Simultaneously transmitting and reflecting reconfigurable intelligent surface (STAR-RIS) assisted UAV communications. *IEEE J. Sel. Areas Commun.* **40**, 3041–3056 (2022)
15. Mondal, A., Biswas, S.: Performance analysis of RIS aided IBFD STAR wireless networks. In: 2022 National Conference on Communications (NCC) (2022)
16. Dhok, S., Sharma, P.K.: Rate-splitting multiple access with STAR RIS over spatially-correlated channels. *IEEE Trans. Commun.* **70**, 6410–6424 (2022)
17. Wang, T., Badiu, M.-A., Chen, G., Coon, J.P.: Outage probability analysis of STAR-RIS assisted NOMA network with correlated channels. *IEEE Commun. Lett.* **26**(8), 1774–1778 (2022)
18. Aldababsa, Mahmoud, Khaleel, Aymen, Basar, Ertugrul: STAR-RIS-NOMA Networks: An Error Performance Perspective, *IEEE Communications Letters*, **26**(8), (2022)
19. Papazafeiropoulos, A., Abdullah, Z., Kourtessis, P., Kisseleff, S., Krikidis, I.: Coverage probability of STAR-RIS-assisted massive MIMO systems with correlation and phase errors. *IEEE Wirel. Commun. Lett.* **11**(8), 1738–1742 (2022)
20. Ni, W., Liu, Y., Eldar, Y.C., Yang, Z., Tian, H.: STAR-RIS integrated nonorthogonal multiple access and over-the-air federated learning: framework, analysis, and optimization. *IEEE Internet Things J.* **9**(18), 17136–17156 (2022)
21. Zhang, Z., Chen, J., Liu, Y., Wu, Q., He, B., Yang, L.: On the secrecy design of STAR-RIS assisted uplink NOMA networks. *IEEE Trans. Wirel. Commun.* **21**, 11207–11221 (2022)
22. Gunasinghe, D., Amarasuriya, G.: Performance analysis of STAR-RIS for wireless communication. In: ICC 2022-IEEE International Conference on Communications (2022)
23. Liu, H., Li, G., Li, X., Liu, Y., Huang, G., Ding, Z.: Effective capacity analysis of STAR-RIS-assisted NOMA networks. *IEEE Wirel. Commun. Lett.* **11**(9), 1930–1934 (2022)
24. Yang, S., Zhang, J., Xia, W., Gao, H., Zhu, H.: Joint power and discrete amplitude allocation for STAR-RIS-aided NOMA system. *IEEE Trans. Veh. Technol.* **71**, 13382–13386 (2022)
25. Papazafeiropoulos, A., Kourtessis, P., Krikidis, I.: STAR-RIS assisted full-duplex systems: impact of correlation and maximization. *IEEE Commun. Lett.* **26**, 3004–3008 (2022)
26. Zuo, J., Liu, Y., Ding, Z., Song, L., Vincent Poor, H.: Joint design for simultaneously transmitting and reflecting (STAR) RIS assisted NOMA systems. *IEEE Trans. Wirel. Commun.* **22**, 611–626 (2022)
27. Chen, J., Yu, X.: Ergodic rate analysis and phase design of STAR-RIS aided NOMA with statistical CSI. *IEEE Commun. Lett.* **26**, 2889–2893 (2022)
28. Xie, Z., Yi, W., Wu, X., Liu, Y., Nallanathan, A.: STAR-RIS aided NOMA in multicell networks: a general analytical framework with gamma distributed channel modeling. *IEEE Trans. Commun.* **70**(8), 5629–5644 (2022)
29. Wang, W., Ni, W., Tian, H.Y., Zhaohui, H., Chongwen, W., Kai-Kit: robust design for STAR-RIS secured internet of medical things. In: 2022 IEEE International Conference on Communications Workshops (ICC Workshops) (2022)
30. Nguyen, T.H., Nguyen, T.T.: On performance of STAR-RIS-enabled multiple two-way full-duplex D2D communication systems. *IEEE Access* **10**, 89063–89071 (2022)
31. Xi, Y., Burr, A., Wei, J.B., Grace, D.: A general upper bound to evaluate packet error rate over quasi-static fading channels. *IEEE Trans. Wirel. Commun.* **10**(5), 1373–1377 (2011)
32. Proakis, J.: *Digital Communications*, 5th edn. Mac Graw-Hill, New York (2007)

**Publisher's Note** Springer Nature remains neutral with regard to jurisdictional claims in published maps and institutional affiliations.

Springer Nature or its licensor (e.g. a society or other partner) holds exclusive rights to this article under a publishing agreement with the author(s) or other rightsholder(s); author self-archiving of the accepted manuscript version of this article is solely governed by the terms of such publishing agreement and applicable law.